Supporting Information

Macrocycle Molecule-based Cryoprotectants for Ice Recrystallization Inhibition and Cell Cryopreservation

Bing Hu,[a,b] Guo-Kai, Li,[a,b] Guo-Min Ai[c], Man Zhang,[a,b] Shan-Shan Su,[a,b] Xu He,[a,b] Xiao-Liu Li,*[a,b] Ke-Rang Wang* [a,b]

[a] College of chemistry and environmental science, Hebei University, Baoding, 071002, P. R. China. E-mail: kerangwang@hbu.edu.cn; lixl@hbu.cn.

[b] Key Laboratory of Medicinal Chemistry and Molecular Diagnosis (Hebei University), Ministry of Education; Key Laboratory of Chemical Biology of Hebei Province, Hebei University, Baoding, 071002, P. R. China.

[c] State Key Laboratory of Microbial Resources, Institute of Microbiology, Chinese Academy of Sciences, Beijing 100101, China.

S1. Experimental section

1.1 Materials and measurements

^{1}H NMR and ^{13}C NMR spectra were recorded on a 400 spectrometer. HRMS analysis was performed on a FT-MALDI MS (Bruker Company). IRI activity analysis was performed on a Nikon polarized optical microscope (LV100ND, Japan) equipped with a Linkman (LTS420) cooling stage. **15C5**, **18C6** and **N-18C6** were purchased from TCI (Shanghai). HPLC was performed with an Agilent 1260 HPLC.

1.2 Ice recrystallization inhibition (IRI) activity

IRI activity analysis was performed via a splat cooling method. The experimental apparatus used to investigate the IRI activity was equipped with a Nikon polarized

optical microscope (LV100ND, Japan) and a Linkman (LTS420) cooling stage. In a typical IRI activity measurement, a 10 μL droplet of solution at room temperature (25 °C) was dropped onto the surface of a silicon substrate precooled to -60.0 °C with liquid nitrogen from a height of 1.5 m. The droplet quickly formed to a thin layer of ice. Then the temperature was increased to -6.0 °C at a rate of 15 °C min^{-1}, and the samples annealed at this temperature for 30 min. The ice wafer was imaged randomly with a digital camera (Nikon Y-TV55, Japan) to obtain the grain size of the ice crystals. Image J software was used to calculate the average number of ice crystals in the fields of four photos, and the mean grain size (MGS) values relative to that of the PBS solution were calculated.

1.3 Dynamic ice shaping (DIS) activity with an improved sucrose-assisted dynamic ice shaping experiment

An improved sucrose-assisted DIS experiment was performed using a Nikon polarized optical microscope (LV100ND, Japan), controlling the temperature with a Linkman LTS 420 cooling stage. Each compound was dissolved in 45.0 wt. % sucrose solution with the final concentrations of 10 mg/mL, 20 mg/mL, and 40 mg/mL, respectively. 45.0 wt. % Sucrose solution was as control group. One microlitre of 45 wt. % sucrose solution was placed in the center of a circle on a microscope slide, then a cover slide was covered, and which was sealed with a flap sealant. The microscope slide was placed on the heating/cooling stage and cooled to -50 °C at a rate of 25 °C/min. The temperature was remained at -50 °C until ice nucleation was formed, followed by heating up to -8 °C at a rate of 5 °C/min, and further warmed up at a rate

of 0.5 °C/min to melt most of the ice crystals. A single ice crystal was observed, then which was cooled at a rate of 0.1 °C/min to a point at which the size of the ice crystals remains constant. After that, the single ice crystal was continued to cool at the same rate of 0.1 °C/min. Photographs of ice crystal shaping was observed at 0.2 °C intervals, and the corresponding growth rate (γ) was calculated.

1.4 Sucrose-sandwich IRI assay

Sucrose-sandwich IRI assay was performed using a Nikon polarized optical microscope (LV100ND, Japan), controlling the temperature with a Linkman LTS 420 cooling stage. Each compound was dissolved in 45.0 wt. % sucrose solution with the final concentrations of 10 mg/mL, 20 mg/mL, and 40 mg/mL, respectively. 45.0 wt. % Sucrose solution was as control group. Samples were dissolved in 45 wt. % sucrose solution, which were sandwiched with two cover slides and sealed with a flap sealant. Samples were cooled to -50°C at a rate of 25 °C/min on a heating/cooling stage, then maintained for 2 min. The temperature was increased to -8 °C at a rate of 5°C/min and held for 60 min. The ice crystal shape was observed.

1.5 Cytotoxicity of macrocycle molecules in human cells

GES-1, hucMSCs and A549 cells were seeded in a 96-well plate at a density of 7 × 10^3 cells per well (with 180 μL of DMEM). After 24 h of incubation, 20 μL of medium containing different concentrations of macrocycle molecules was added to the wells with cells. Then, all the cells were cultured for an additional 48 h. Cell viability was assessed by the MTT method. First, cells were incubated with MTT (0.5 mg mL^{-1}) for 4 h at 37 °C. During this incubation period, water-insoluble crystals

formed, which were then dissolved by the addition of 100 μL of a hydrochloric acid-isopropanol mixed solution to each well. The optical density at 490 nm in each well was measured using an enzyme-linked immunosorbent assay plate reader. Wells containing culture medium and MTT but no cells acted as blanks. The percent of cell viability was calculated as follows: $(A_{compound} - A_{blank})/(A_{control} - A_{blank}) \times 100\%$.

1.6 Cryopreservation of human cells

GES-1, hucMSCs and A549 cells were cultured under standard conditions (5% CO_2, 37 °C). GES-1, hucMSCs and A549 cells were grown in DMEM supplemented with 10% FBS. After 48 h of incubation under standard conditions (5% CO_2, 37 °C), the cells were washed from the plate using trypsin and centrifuged for 3 min at 1200 rpm. For cryopreservation, the cells were diluted into the cryoprotectants (87.5% DMEM, 10% FBS and 2.5% DMSO) containing different concentrations of macrocycle molecules (0.25, 0.5 and 1.0 mg/mL) at a density of 5×10^5 cells·mL^{-1}. The mixtures were first cooled from room temperature to 4 °C and equilibrated for 5 min. Then, they were further frozen in a -20 °C freezer and equilibrated for 0.5 h. Finally, the mixtures were frozen in a -80 °C freezer and equilibrated for 24 h to completely freeze the cells. To thaw the cells, the mixtures were placed in a water bath at 37 °C for 2 min. After removing of the cryoprotectants, the cells were cultured in DMEM with 10% FBS under standard conditions. After 24 h of incubation, adherent cells (alive) were counted, and the proportion of surviving cells compared to the total number of cells was calculated and compared with the group without compound. Six parallels in each group were repeated three times.

On the other hand, post-thaw cell proliferation was evaluated after incubation for 24 h and typical thawing as the above described procedure. Light microscope images were performed to observe the live cells.

1.7 Melting points of the cryoprotectant solutions

α-TMCD (0.5 mg/mL) was dissolved in PBS buffer with and without DMSO (2.5%). The PBS buffer was as a control group. The range of the melting temperature is determined by a Nikon polarized optical microscope (LV100ND, Japan). The temperature was controlled by a Linkman LTS 420 cooling stage. One microlitre of solution was deposited in the center of a circle on a microscope slide, which was covered with a cover slide and sealed with a flap sealant. The melting temperature was determined under the heating rates of 5 °C·min^{-1} and 10 °C·min^{-1}, respectively. The initial melting temperature and the complete melting temperature were recorded, respectively.

1.8 Cellular uptake assay

A549 cells were seeded in 6-well plates at a concentration of 2.5×10^5 cells per well, and the culture medium containing 0.5 mg/mL α-TMCD with and without DMSO (2.5%) was added, which was incubated at 37 °C and 5% CO_2 for 24 h. after that, the culture medium was removed, washed three times with PBS buffer, and 1 mL of deionized water was added to the medium, the cells were collected, filtered and lyophilized. The content of α-TMCD were studied with a HPLC-MS experiment.

1.9 NMR and HRMS results

α-TMCD: ^{1}H NMR ($CDCl_3$, 400 MHz): δ 5.06 (d, J = 2.8 Hz, 6H), 3.85-3.79 (12H), 3.71-3.69 (6H), 3.65 (s, 18H), 3.61-3.52 (12 H), 3.49 (s, 18H), 3.41 (s, 18H), 3.19 (dd, J = 2.4, 9.6 Hz, 6H); ^{13}C NMR ($CDCl_3$, 100 MHz): δ 57.84, 58.98, 61.80, 71.22, 71.46, 81.25, 82.22, 82.48, 100.14; HRMS (FTMS): calcd for $C_{54}H_{96}NaO_{30}$, 1247.5878, found, 1247.5873.

β-TMCD: ^{1}H NMR ($CDCl_3$, 400 MHz): δ 5.13 (d, J = 3.6 Hz, 7H), 3.85-3.79 (14H), 3.64 (s, 31H), 3.61-3.57 (14H), 3.53-3.48 (28H), 3.38 (s, 21H), 3.21 (dd, J =

3.6, 10.0 Hz, 7H); ^{13}C NMR ($CDCl_3$, 100 MHz): δ 58.53, 58.56, 59.02, 61.48, 61.51, 70.94, 71.42, 80.34, 81.78, 82.07, 98.99; HRMS (FTMS): calcd for $C_{63}H_{112}NaO_{35}$, 1451.6876, found, 1451.6863.

γ-TMCD: ^{1}H NMR ($CDCl_3$, 400 MHz): δ 5.24 (d, J = 3.6 Hz, 8H), 3.87 (dd, J = 3.2, 10.4 Hz, 8H), 3.77-3.66 (16H), 3.65 (s, 24H), 3.57-3.52 (16H), 3.51 (s, 24H), 3.37 (s, 24H), 3.23 (dd, J = 3.6, 9.6 Hz, 8H); ^{13}C NMR ($CDCl_3$, 100 MHz): δ 58.70, 58.73, 59.01, 59.05, 61.40, 61.43, 70.94, 71.29, 81.94, 82.01, 98.05; HRMS (FTMS): calcd for $C_{72}H_{128}NaO_{40}$, 1655.7874, found, 1655.7859.

S2. Additional figures

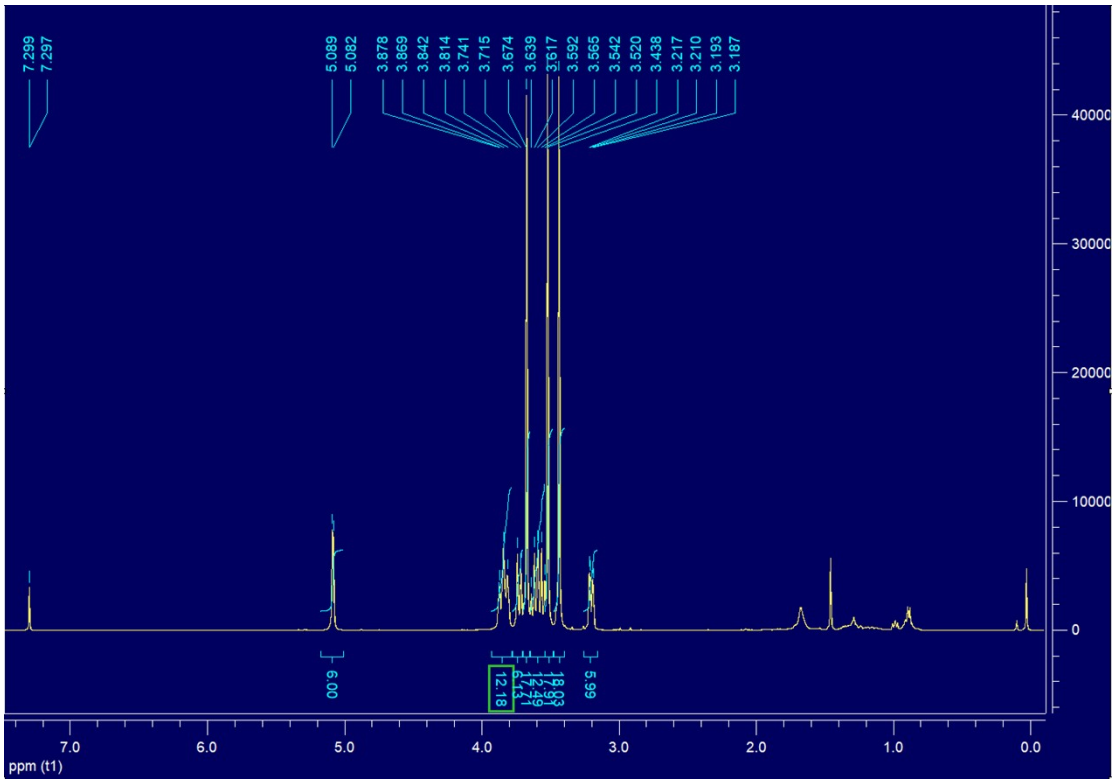

Fig. S1 ^{1}H NMR ($CDCl_3$, 400 MHz) of **α-TMCD**.

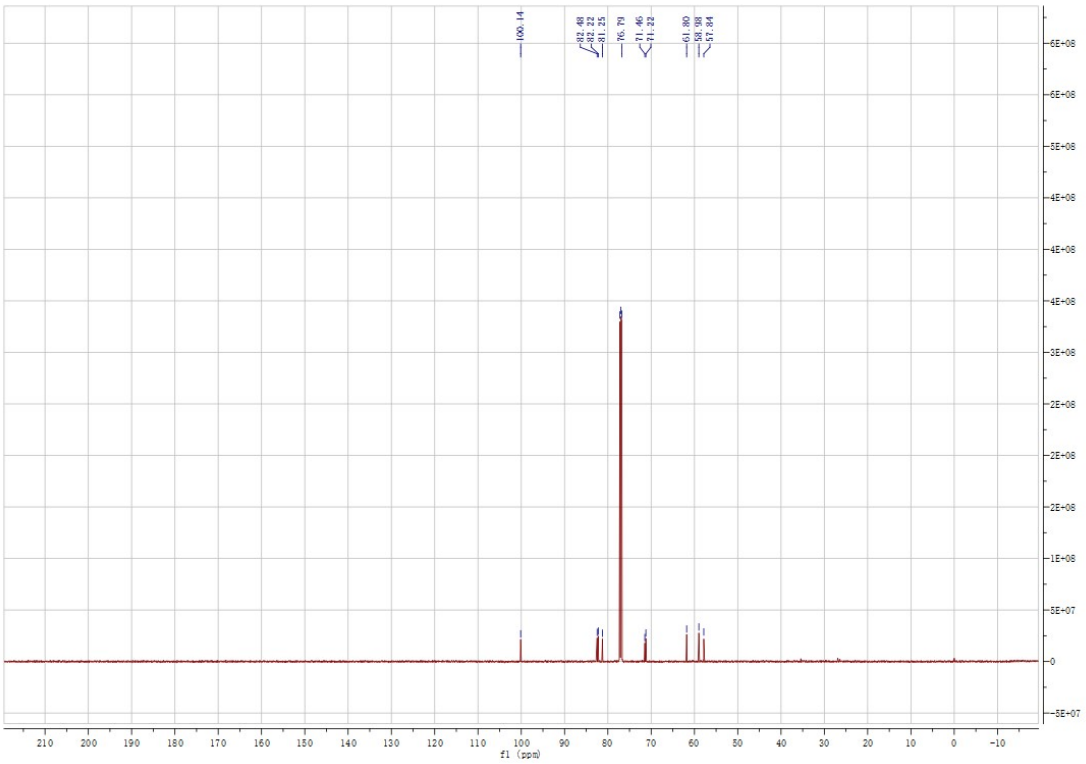

Fig. S2 ^{13}C NMR ($CDCl_3$, 100 MHz) of **α-TMCD**.

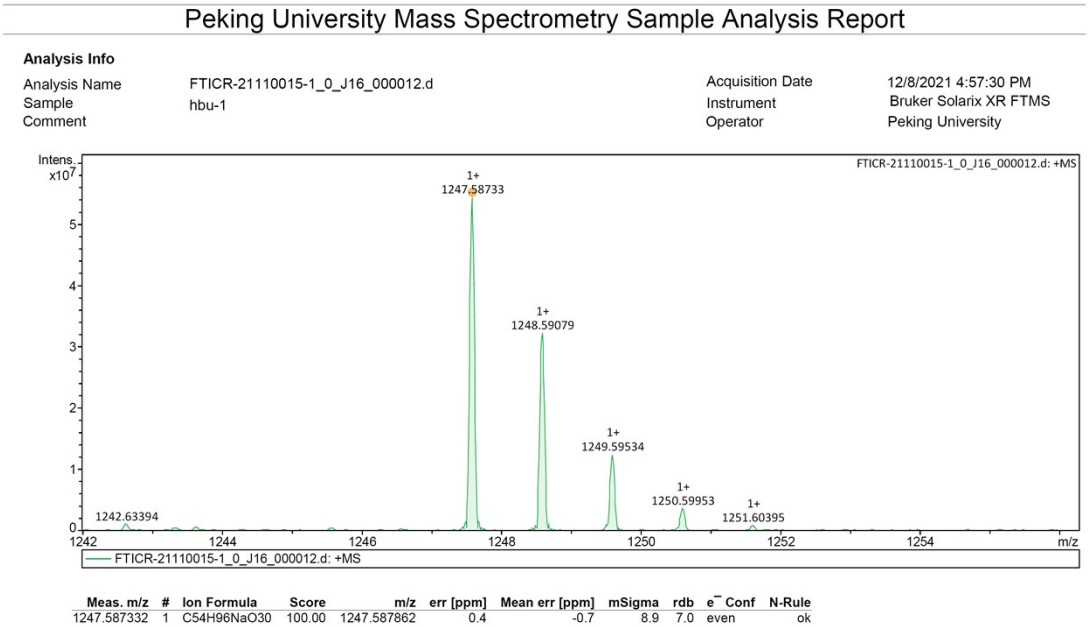

Fig. S3 HRMS (FTMS) of **α-TMCD**.

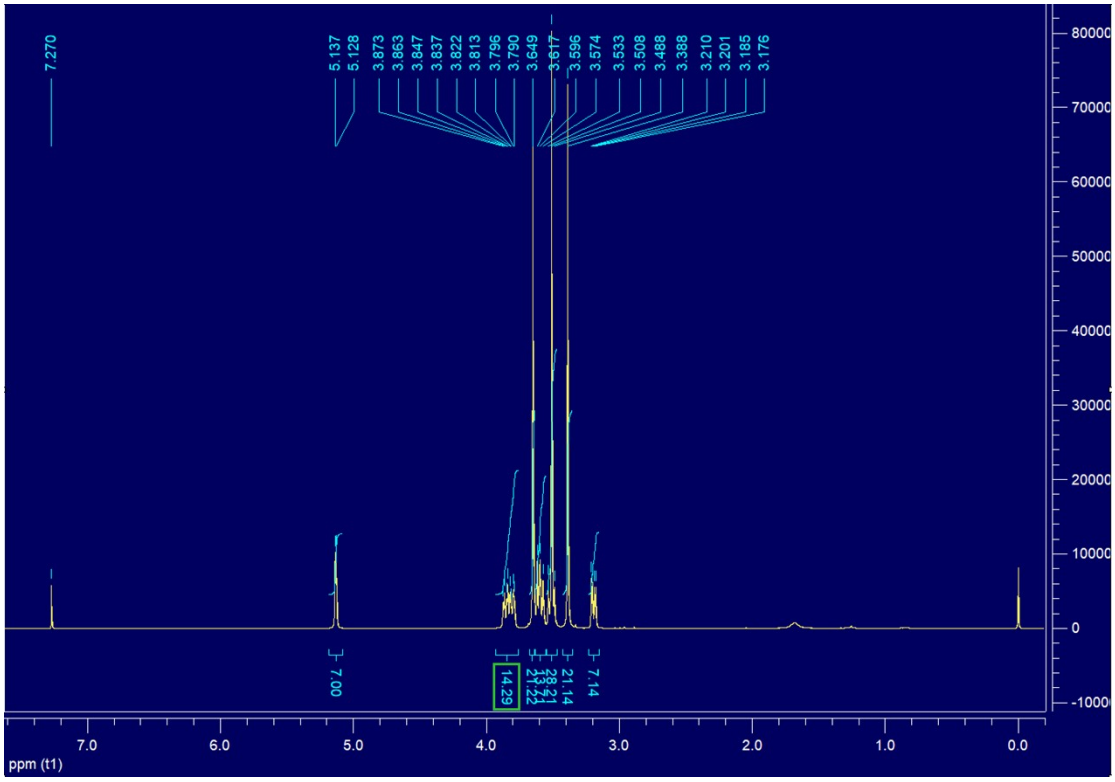

Fig. S4 ^{1}H NMR ($CDCl_3$, 400 MHz) of **β-TMCD**.

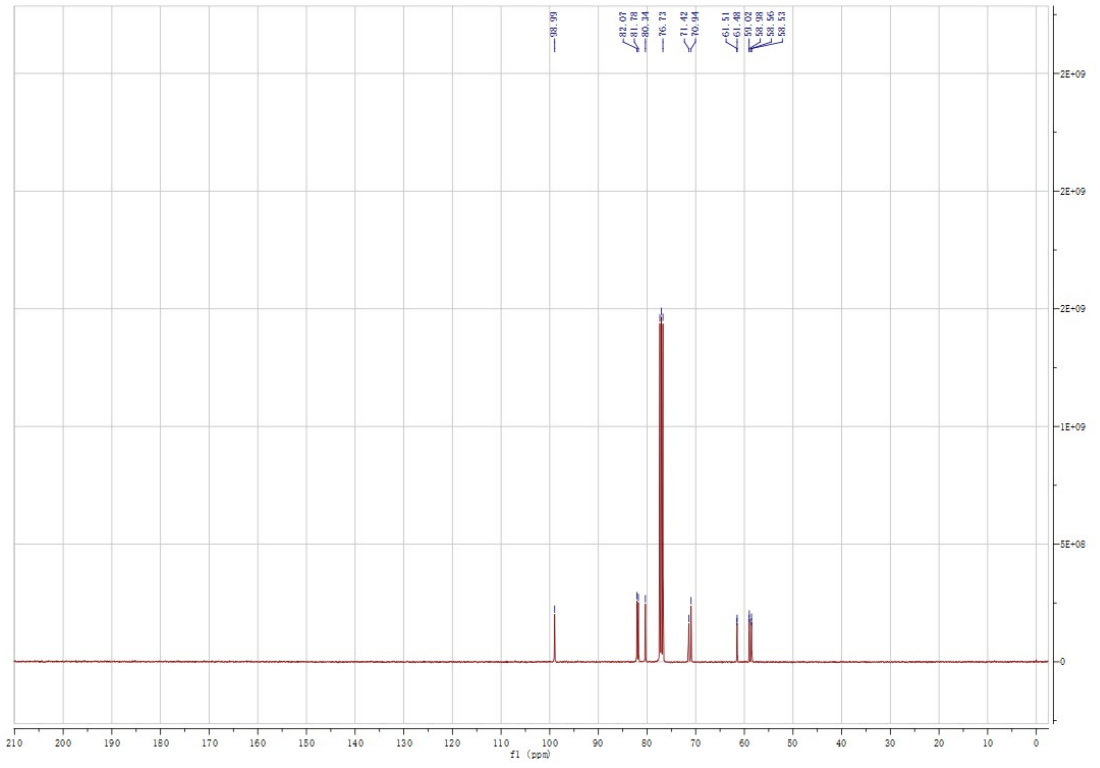

Fig. S5 ^{13}C NMR ($CDCl_3$, 100 MHz) of **β-TMCD**.

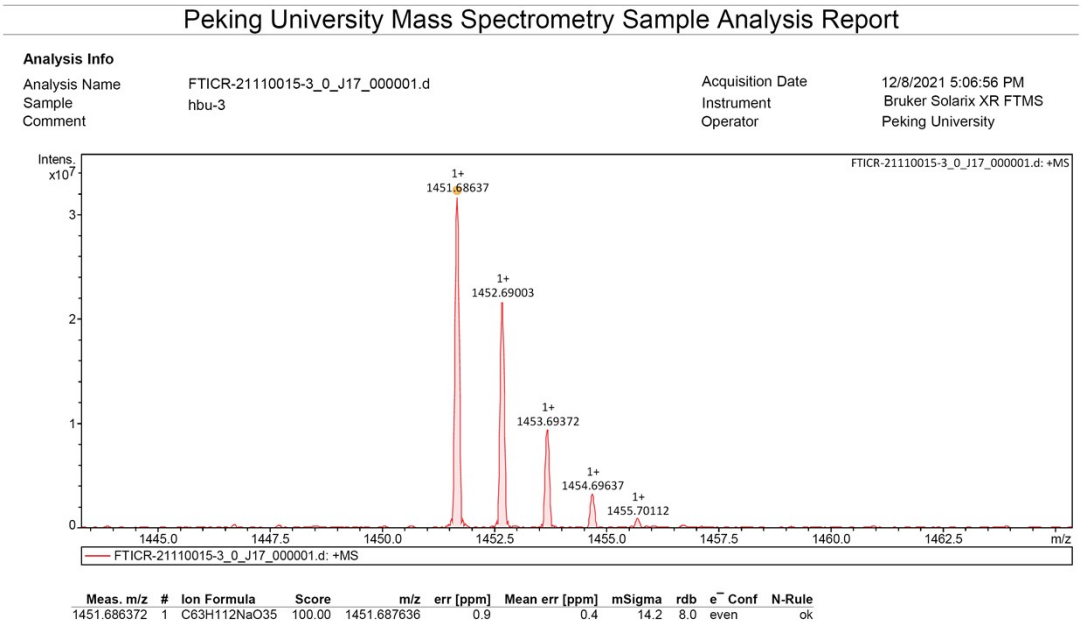

Fig. S6 HRMS (FTMS) of **β-TMCD**.

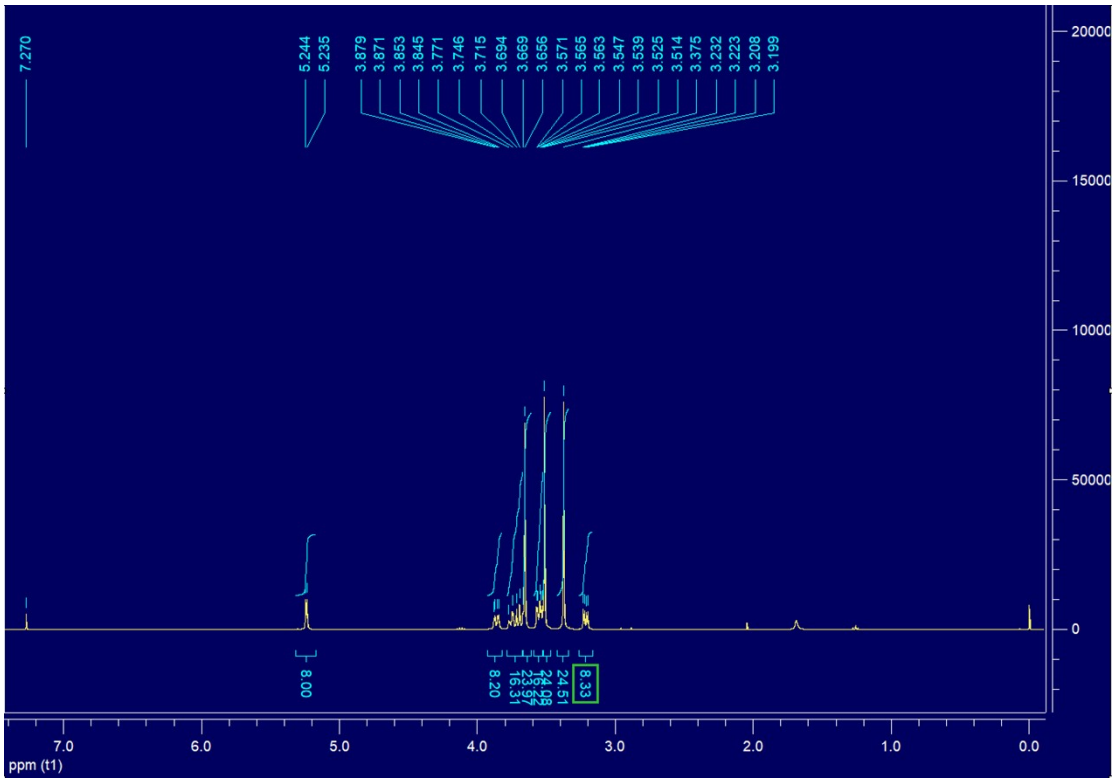

Fig. S7 ^{1}H NMR ($CDCl_3$, 400 MHz) of **γ-TMCD**.

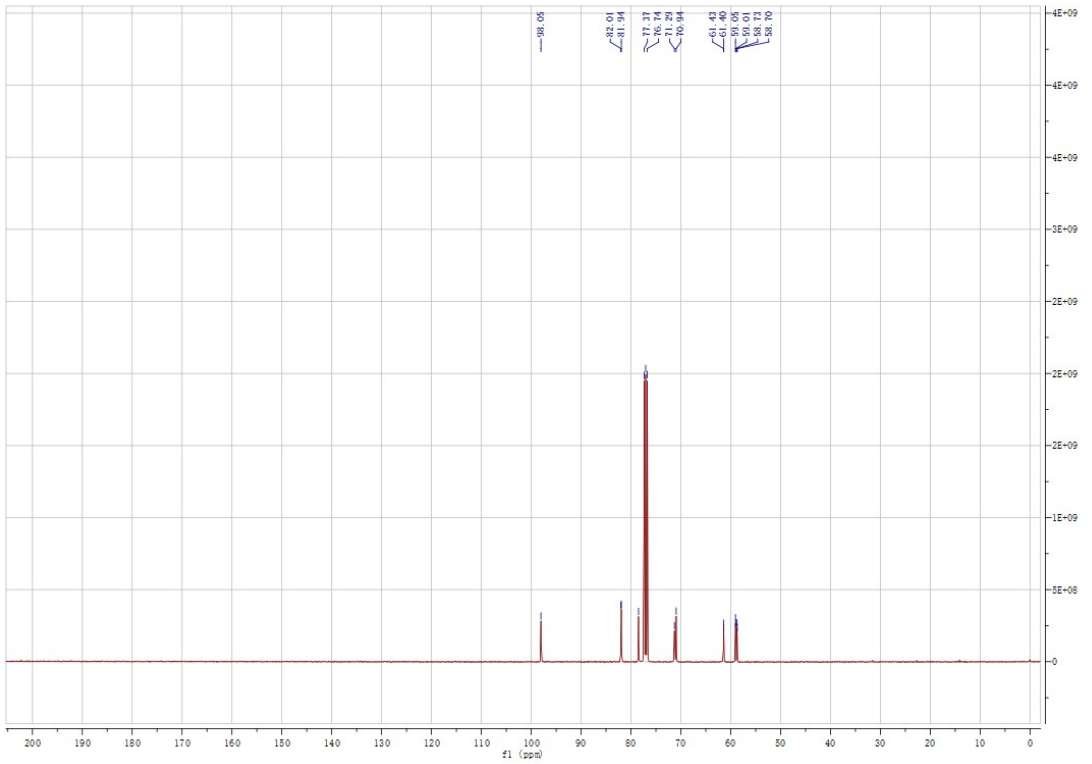

Fig. S8 ^{13}C NMR ($CDCl_3$, 100 MHz) of **γ-TMCD**.

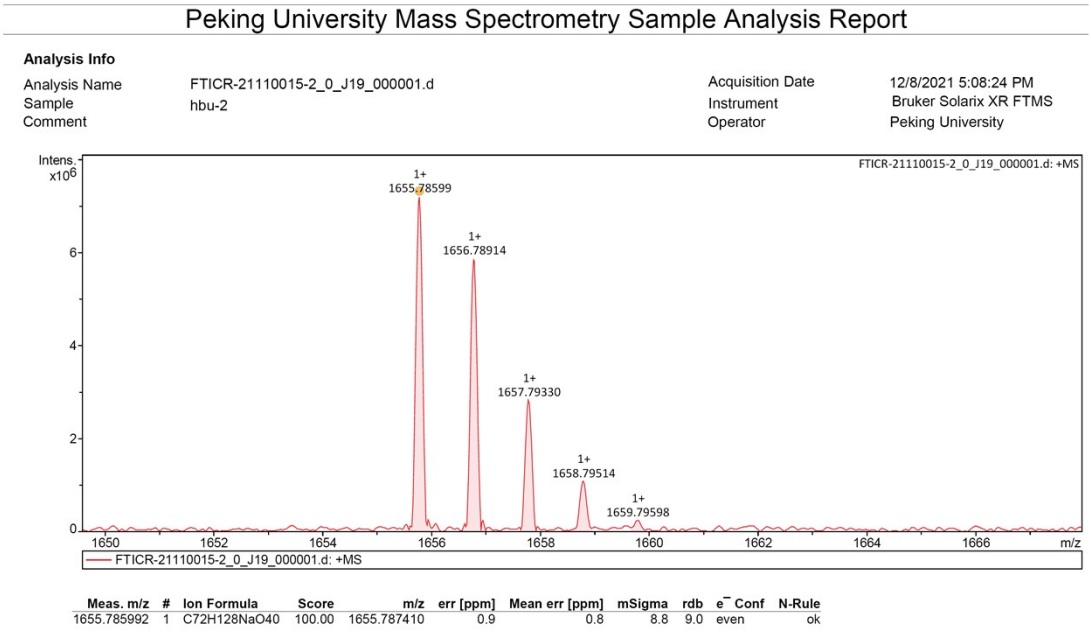

Fig. S9 HRMS (FTMS) of **γ-TMCD**.

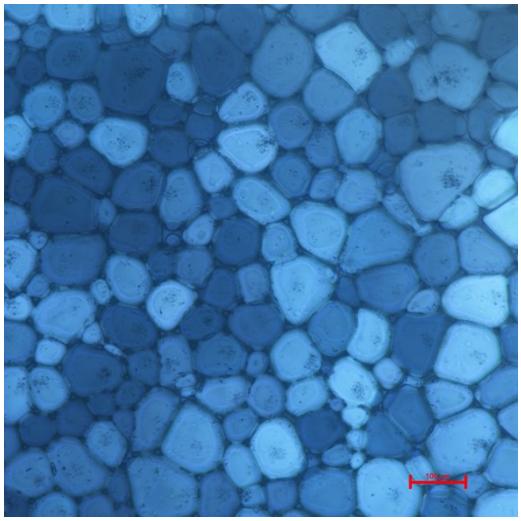

Fig. S10 Representative polarized light microscopy images of ice wafers for PBS buffer (pH = 7.3) after 30 min annealing at -6 °C.

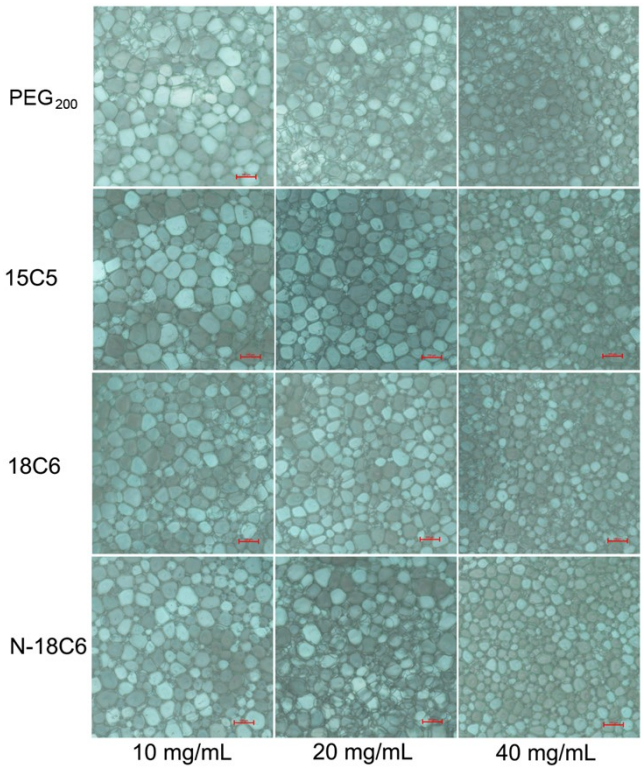

Fig. S11 Representative polarized light microscopy images of ice wafers for **PEG_{200}**, **15C5**, **18C6** and **N-18C6** after 30 min annealing at -6 °C under the concentrations of 10 mg/mL, 20 mg/mL and 40 mg/mL in the solution of PBS buffer (pH = 7.3).

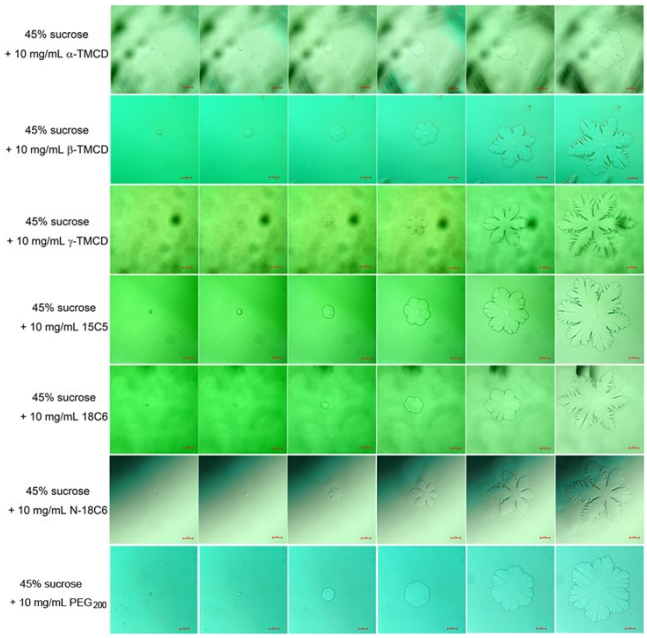

Fig. S12 Sucrose-assisted DIS experiment of macrocycle molecules (10 mg/mL) along with 45 wt. % sucrose.

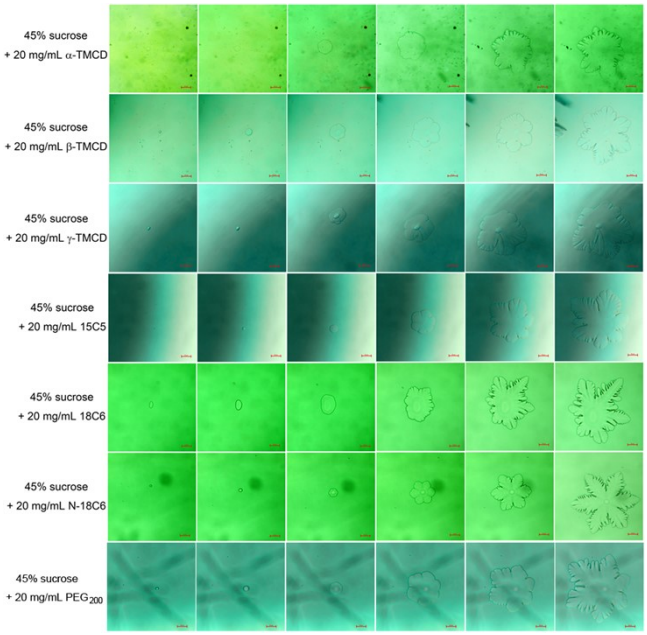

Fig. S13 Sucrose-assisted DIS experiment of macrocycle molecules (20 mg/mL) along with 45 wt. % sucrose.

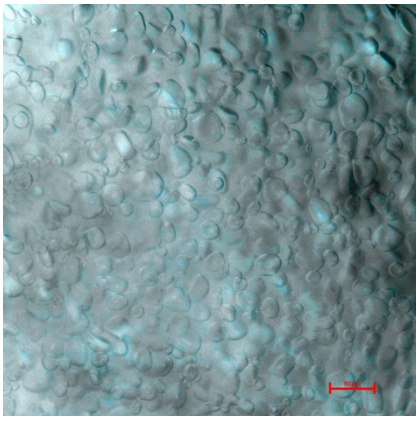

Fig. S14 Microphotograph of 45 wt. % sucrose annealed at -8.0 °C for 60 min.

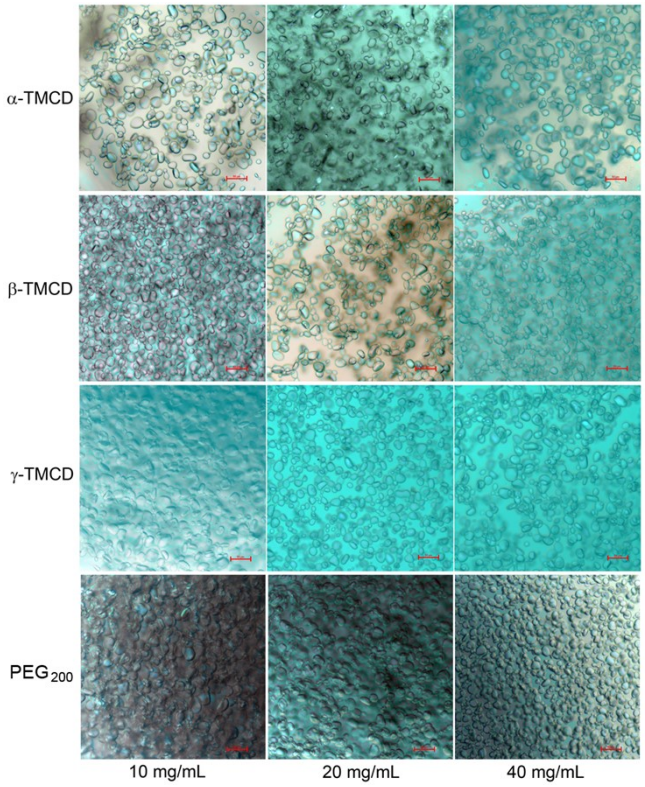

Fig. S15 Microphotographs of 45 wt. % sucrose annealed at -8.0 °C for 60 min with different concentrations (10, 20 and 40 mg/mL) of **α-TMCD**, **β-TMCD**, **γ-TMCD** and **PEG_{200}**.

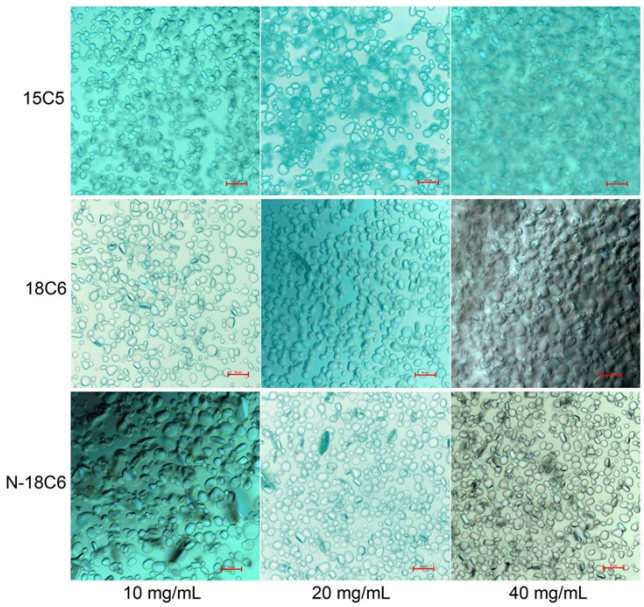

Fig. S16 Microphotographs of 45 wt. % sucrose annealed at -8.0 °C for 60 min with different concentrations (10, 20 and 40 mg/mL) of **15C5**, **18C6** and **N-18C6**.

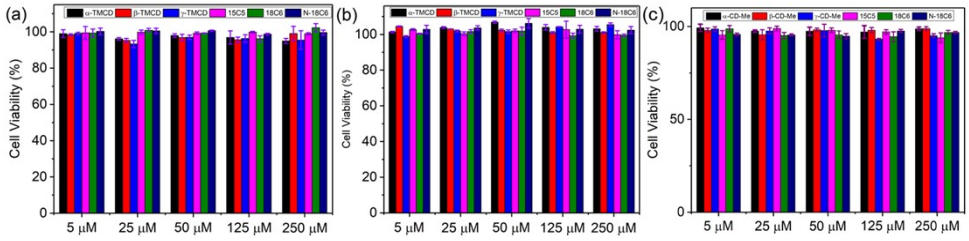

Fig. S17 Cell viability of the macrocycle supramolecular molecules (**α-TMCD**, **β-TMCD**, **γ-TMCD**, **15C5**, **18C6** and **N-18C6**) against GES-1 (a), hucMSCs cells (b) and A549 (c) cells at different concentrations (5.0, 25.0, 50.0, 125.0 and 250.0 μM). Each value represents the mean ± SEM (n = 6).

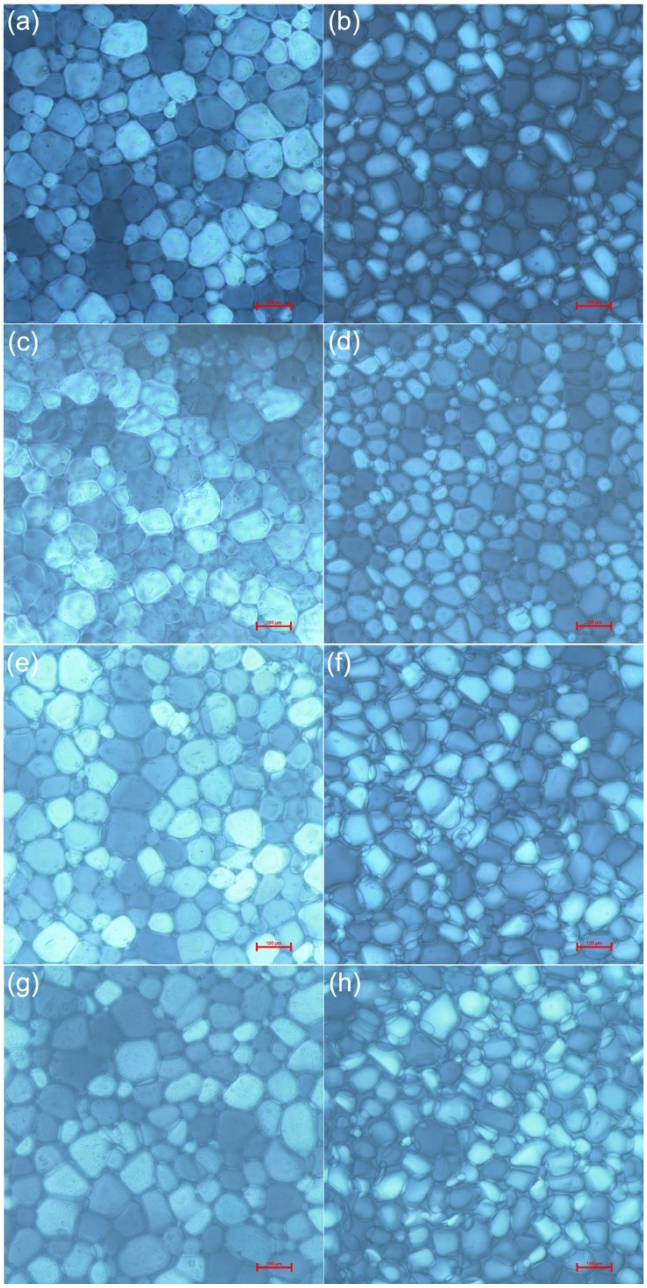

Fig. S18 Representative polarized light microscopy images of ice wafers for PBS buffer group (a, control), 2.5% DMSO (b), **α-TMCD** (0.5 mg, c), **α-TMCD-DMSO** (0.5 mg-2.5%, d), **β-TMCD** (0.5 mg, e), **β-TMCD-DMSO** (0.5 mg-2.5%, f), **γ-TMCD** (0.5 mg, g) and **γ-TMCD-DMSO** (0.5 mg-2.5%, h) after 30 min annealing at -6 °C.